# Articular Cartilage Deformation Determined in an Intact Tibiofemoral Joint by Displacement-Encoded Imaging

Deva D. Chan,[1,2] Corey P. Neu,[2*] and Maury L. Hull[1,3]

**This study demonstrates the in vitro displacement and strain of articular cartilage in a cyclically-compressed and intact joint using displacement-encoded imaging with stimulated echoes (DENSE) and fast spin echo (FSE). Deformation and strain fields exhibited complex and heterogeneous patterns. The displacements in the loading direction ranged from −1688 to −1481 μm in the tibial cartilage and from −1601 to −764 μm in the femoral cartilage. Corresponding strains ranged from −9.8% to 0.7% and from −4.3% to 0.0%. The displacement and strain precision were determined to be 65 μm and less than 0.2%, respectively. Displacement-encoded magnetic resonance imaging is capable of determining the nonuniform displacements and strains in the articular cartilage of an intact joint to a high precision. Knowledge of these nonuniform strains is critical for the in situ characterization of normal and diseased tissue, as well as the comprehensive evaluation of repair constructs designed using regenerative medicine. Magn Reson Med 61:989–993, 2009.**


**Key words: magnetic resonance imaging; displacement encoding; articular cartilage deformation; tibiofemoral joint; strain**

The measurement of articular cartilage deformation patterns in the intact tibiofemoral joint in vitro can provide unique information regarding degenerative joint diseases. Comparison of deformations from degenerated and healthy knees may elucidate mechanisms of osteoarthritis progression. Knowledge of deformation patterns in whole joints in vitro would be advantageous in the design and evaluation of engineered or repaired cartilage (1,2) and in the development and validation of mathematical models of intact joints. Additionally, as a step toward in vivo measurements, the characterization of articular cartilage deformation in whole joints in vitro is necessary.

MRI has the potential to noninvasively measure articular cartilage deformation in an intact joint. MRI techniques to determine tissue displacement were initially developed to study myocardial deformation (3–5). Among MR studies of orthopedic tissue deformation, spoiled gradient recalled acquisition was used to measure change in cartilage contact area (6), and fast low-angle shots were used to compare cartilage thickness before and after compression (7–9). These measures, however, are not indicative of the heterogeneous deformations occurring within the tissue of interest.

Displacement-encoded imaging with stimulated echoes and fast spin echo readout were previously combined (DENSE-FSE) for measurement of heterogeneous displacements at a precision below the image spatial resolution in bovine articular cartilage explants (10). Although deformation patterns were determined in explants, it is unclear whether patterns observed are meaningful in the context of joint loading, where multiple tissue contacts and complex geometry may result in unexpected deformations. Therefore, the present work extends the previous technique to compute displacement and strain patterns in the articular cartilage of a compressed and intact tibiofemoral joint. To this end, a loading apparatus was designed to cyclically compress an intact joint within an MRI scanner. The first objective was to evaluate the precision of the DENSE-FSE technique with an imaging phantom. A second objective was to demonstrate the in-plane deformation of articular cartilage in an intact tibiofemoral joint, which was expected to be heterogeneous.

## METHODS

Stifle (knee) joints from 1- to 3-month-old porcine were obtained from a local abattoir and frozen at time of harvest. The synovial capsule remained intact for all experiments. At the time of testing, joints were thawed to room temperature and the distal tibia and proximal femur were potted in tubes designed to fit in the loading apparatus (discussed subsequently) using polymethylmethacrylate.

### Apparatus Design and Cyclic Joint Loading

A loading apparatus was designed to apply cyclic compressive loads to a whole joint specimen within an MRI system (Fig. 1). Joint loading was achieved with a double-acting pneumatic cylinder controlled by an electropneumatic system (11). The piston rod transferred load through the tibia in the direction of the femur. The loading apparatus was predominantly constructed from plastic; no metal components were present in the radio frequency coil. When placed in the MRI scanner, the apparatus held the specimen joint line at the magnet isocenter. The relationship between regulator input voltage and applied load was measured with a load cell (LC307-250; Omega Engineering, Inc., Stamford, CT).

To allow for the acquisition of data over time, the specimen was cyclically compressed, and imaging was not performed until a quasi-steady state load-deformation response was achieved. The number of cycles required to reach quasi-steady state was found for loads of one-times

[1]Biomedical Engineering Graduate Group, University of California at Davis, Davis, California.

[2]Weldon School of Biomedical Engineering, Purdue University, West Lafayette, Indiana.

[3]Department of Mechanical and Aeronautical Engineering, University of California at Davis, Davis, California.

Grant sponsor: National Institutes of Health; Grant number: NIBIB 1F32 EB003371-01A1; Grant sponsor: UC Davis NMR facility.

*Correspondence to: Corey P. Neu, Weldon School of Biomedical Engineering, Purdue University, 206 S. Martin Jischke Drive, West Lafayette, IN 47907-2032. E-mail: cpneu@purdue.edu

Received 30 June 2008; revised 15 October 2008; accepted 19 November 2008.

DOI 10.1002/mrm.21927

Published online 2 February 2009 in Wiley InterScience (www.interscience.wiley.com).

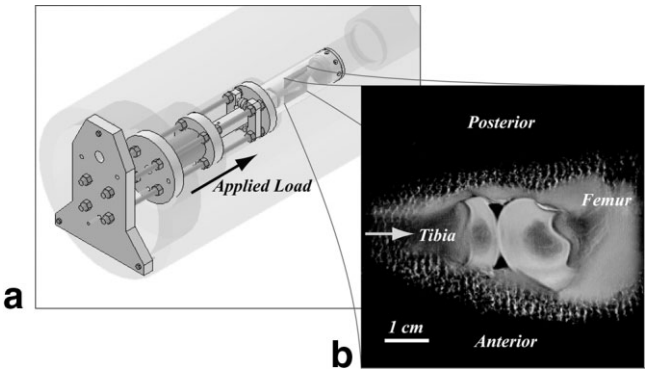


FIG. 1. The loading apparatus (**a**) allowed for cyclic compression of an intact cadaveric tibiofemoral joint inside an MRI scanner. The gray overlay indicates the bore of the system and highlights the design constraints of the loading apparatus. The gray square indicates how the image slice is oriented with respect to the loading apparatus. A sample proton-weighted image is presented (**b**) to demonstrate the anatomical position of a tibiofemoral joint within the loading apparatus. Loading is applied through the tibia in the distal-to-proximal direction to the femur, as indicated by the arrows.

body weight (78 N) (12), which are typical of tibiofemoral joints during the quadruped gait cycle (13), using 11 specimens. Load was applied for 1.5 s during each 10-s cycle (11). These tests occurred outside the MR scanner to allow for the use of a laser displacement sensor (LB-081/1101(W), Keyence Corporation, Woodcliff Lake, NJ) to measure the displacement of the tibia relative to the loading apparatus, to which the femur was fixed. The load-deformation response was considered to have reached quasi-steady state when the linearly time-regressed slope of displacement fell below the predetermined-slope criterion (11). This criterion, half the spatial resolution divided by the total imaging time, was 0.0163 μm/s, based on a spatial resolution of 250 μm and the 768 ten-s cycles required for image acquisition (total imaging time = 128 min).

### Displacement-Encoded Imaging

Changes in displacement Δx can be computed from DENSE-FSE phase data Δϕ (10) according to the following relation:

$$\Delta\varphi = \gamma_H t_{enc}(G_{de} - G'_{de})\Delta x \qquad [1]$$

where $\gamma_H$ is the gyromagnetic ratio of $^1$H, $t_{enc}$ is the effective gradient encoding duration, $G_{de}$ is the gradient magnitude for displacement encoding, and $G'_{de}$ is the gradient magnitude for reference data, which was used to eliminate phase contributions common to all images. Although the equation above does not include the influence of eddy currents on phase information, previous studies (10) indicate that eddy currents have only a small or negligible influence on the present work.

The DENSE-FSE pulse sequence was implemented in a horizontal-bore Bruker Biospec 70/30 system (7.05 Tesla; Bruker Medical GMBH, Ettlingen, Germany). The DENSE-FSE imaging parameters were: $t_{enc}$ = 2.9 ms, $G_{de}$ = 4.75 mT/m for frequency- and phase-direction displacement encoding, and $G'_{de}$ = 0 mT/m for the reference image. Imaging parameters for the intact joint were: effective repetition time = 10,000 ms; echo time = 8.7420 ms; bandwidth = 101 kHz; field of view = 64 × 64 mm; slice thickness = 2 mm; matrix size = 256 × 256 pixels; number of echoes per excitation = 16; number of averages = 4. Additionally, cosine and sine modulation to eliminate artifacts required that four phase-modulated acquisitions of the same slice be combined for elimination of anti-echo and $T_1$ decay artifacts (14). An electrical trigger from the electropneumatic system to the MR scanner ensured that each pulse sequence occurred during the same portion of the loading cycle. Displacement-encoding gradient occurred before and during load application, and FSE readout occurred during the loading plateau (Fig. 2).

### Image Analysis

Regions of interest representing the tibial and femoral cartilage were segmented using commercial software (Paravision, Bruker Medical GMBH, Ettlingen, Germany). Image analysis of these regions was performed using MATLAB (v.7.0, The Mathworks, Natick, MA). For each scan, phase-modulated data were combined (14) and a two-dimensional inverse Fourier transform was applied. First-order phase correction was performed on the reference scan and applied to the displacement-encoded images. The phase, which was accumulated during the motion of the specimen in the time interval between the two applied displacement-encoded gradients, was unwrapped.

Displacements were determined by subtraction of the reference phase contribution from the phase in the frequency- and phase-encode directions and subsequent conversion of the phase data into displacement fields in the loading and transverse directions, respectively, using Equation [1]. To smooth the displacement field, each point and the neighboring points that fell within the region of

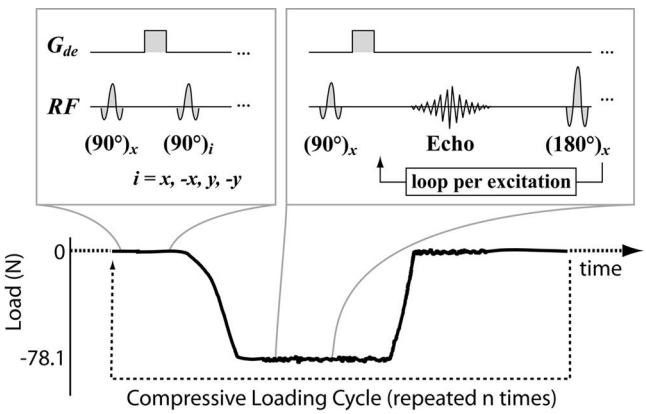


FIG. 2. MRI and loading apparatus integration required precise timing actions. The direction of the second 90° radio frequency (RF) pulse was modulated for artifact elimination. The displacement-encoded gradient ($G_{de}$) is applied between the first two 90°-RF pulses and also after the third 90° RF pulse. Fast spin echo (FSE) acquisition occurred during the loaded portion of each cycle and the displacement-encoded phase information was acquired from a deformed specimen. Timing events are not to scale.

interest were averaged iteratively, using parameters discussed below. Strain fields were computed from the discrete displacement fields using a maximum likelihood estimation of the deformation gradient tensor (10,15). Displacements of a local pixel group were used to calculate the Green-Lagrange strain. Additionally, the signal-to-noise ratio was determined by dividing the average of the signal within the regions of interest by the average noise in image regions that were void of tissue.

### Evaluation of Precision

An elastic silicone phantom (Sylgard-527 dielectric gel; Dow Corning, Midland, MI) was used to evaluate the precision of this technique. Imaging and cyclic loading parameters were identical to those above except for: effective repetition time = 3000 ms; load = 8 N. Nine sequential data acquisitions of reference and displacement-encoded scans were performed and analyzed using the aforementioned techniques. Neighboring pixels were weighted at 1.0, 0.5, 0.25, 0.1, 0.05, or 0.025, with the weight of the pixel of interest at 1.0, for 1, 2, 3, 4, 5, 10, 25, 50, 100, 250, 500, or 1000 cycles of smoothing. The smoothed displacements and strains were computed at nine separate locations to characterize deformations throughout the phantom interior. The precision for displacement and strain data was computed as the pooled standard deviation (of the nine locations and the repeated data acquisitions) for each combination of neighboring pixel weights and cycles of smoothing.

### Demonstration of DENSE-FSE in an Intact Joint

A single juvenile porcine stifle was imaged using the parameters described previously. The imaged slice lay in the sagittal plane, through the tibiofemoral contact area in the medial condyle. Reference and displacement-encoded scans in the frequency and phase directions were acquired using the DENSE-FSE pulse sequence after a quasi-steady state load-deformation response was achieved. Image analysis as described above was then used to calculate the displacement and strain fields in the imaged slice. To smooth the displacement field, a weight of 1.0 was used for 100 iterations.

### Statistics

All data are presented as mean ± standard deviation unless otherwise specified. The relationship between input voltage to the pneumatics system and the resulting applied load was modeled using a linear regression equation and an $R^2$ correlation statistic was computed using Excel (v.11.3.7, Microsoft Corp., Redmond, WA).

## RESULTS

### Apparatus Evaluation and Cyclic Joint Loading

The loading apparatus showed a consistent linear relationship between input voltage and measured applied load ($R^2 = 0.9998$; $P < 0.001$). A quasi-steady state load-displacement response was achieved in intact tibiofemoral joints (Fig. 3). Fresh-frozen juvenile porcine stifles cyclically loaded at 1-times body weight required 224 ± 161 cycles (n = 11) to reach quasi-steady state. Once quasi-steady state was achieved, the standard deviation of displacement during the loaded portion of the cycle was 70.4 ± 29.3 μm (n = 11), less than half the spatial resolution. Therefore, at least 546 (= 224 +(2 × 161)) cycles were applied to the specimen before imaging.

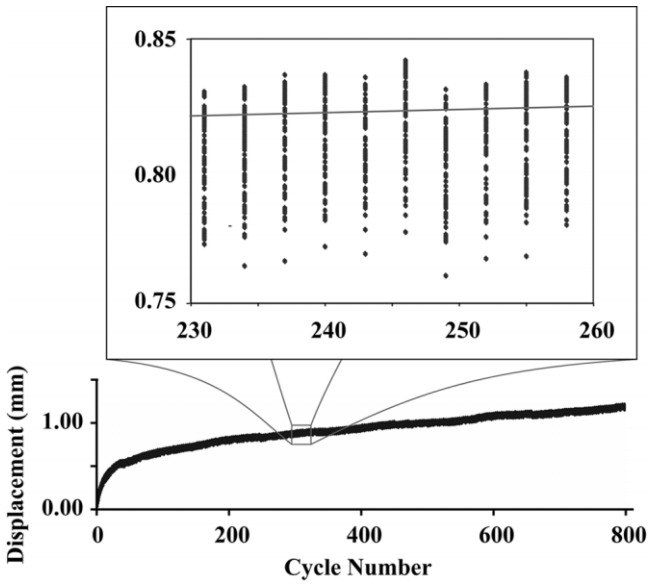


FIG. 3. Quasi-steady state behavior was found to occur after 224 ± 161 cycles over all 11 specimens. The number of cycles to quasi-steady state load-deformation behavior was determined to be 231 for the representative specimen data shown here. Displacements occurring during the loading plateau were used to find the slope of displacement over time, and quasi-steady state was defined when this slope fell below a predetermined criterion (11). The standard deviation of displacement after quasi-steady state was reached was less than half the spatial resolution of imaging.

### Evaluation of Precision

Displacement and strain precisions were measured in repeated tests of the silicone phantom and depended on the smoothing parameters. Before smoothing, the absolute displacement and strain precisions were 132 μm and 77%, respectively. Displacement precision improved with number of smoothing cycles, reaching a plateau at 65 μm, and stronger averaging weights of neighboring pixels produced more precise strains. With the weight at 1.0, displacement precision of 65 μm and strain precision of 0.2% was achieved after 100 smoothing cycles (Fig. 4).

### Demonstration of DENSE-FSE in an Intact Joint

Heterogeneous cartilage deformation and strain patterns were observed in a single intact joint during cyclic loading (Fig. 5). Displacements in the tibial articular cartilage ranged from −1688 to −1481 μm in the loading direction and 55 to 334 μm in the transverse direction. Femoral articular cartilage displacements were between −1601 and −764 μm in the loading direction and 865 and 1378 μm in the transverse direction. The strains in the femoral articular cartilage ranged from −9.8% to 0.7% in the loading

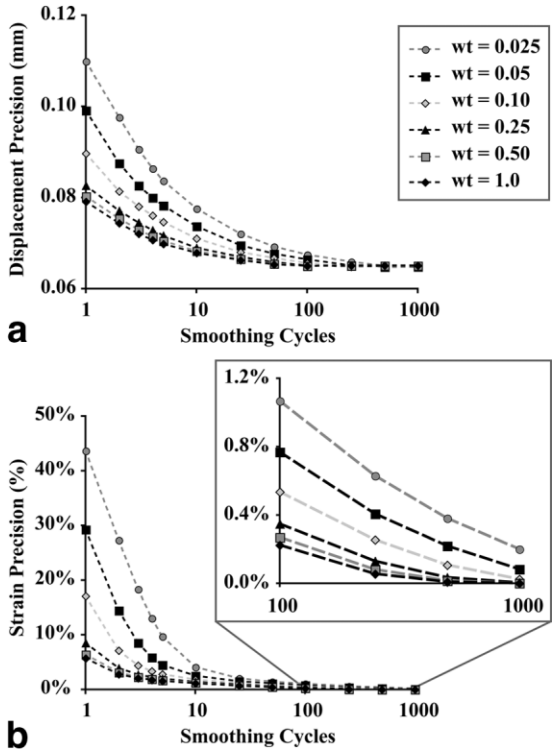


FIG. 4. Precisions in displacement (**a**) and strain (**b**) were improved following data smoothing. Displacements were smoothed 1, 2, 3, 4, 5, 10, 25, 50, 100, 250, 500, and 1000 times using a weighted average, in which neighboring points were given weights (wt) of 1, 0.5, 0.25, 0.10, 0.05, and 0.025. Absolute precision of displacements improved with smoothing cycles until reaching a plateau of 65 μm at approximately 100 cycles. Absolute precision of strains improved with smoothing but did not reach a plateau even after 1000 cycles of smoothing.

direction, −2.3% to 8.5% in the transverse direction, and −4.5% to 3.6% in shear. In the tibial articular cartilage, the strains were −4.3% to 0.0% in the loading direction, 0.0% to 4.8% in the transverse direction, and −0.8% to 1.2% in shear. The signal-to-noise ratio of the tibiofemoral cartilage was 8.17.

## DISCUSSION

This study demonstrated the use of displacement-encoded MR imaging to determine nonuniform displacements and strains in the articular cartilage of an intact joint. A loading apparatus was designed for use inside an MRI scanner, and a porcine tibiofemoral joint was cyclically compressed to a quasi-steady state load-deformation response before imaging. Additionally, the displacement and strain precisions of the technique were estimated using a silicone phantom.

Factors in the choice of a juvenile porcine tibiofemoral joint included space constraints of the MRI scanner and the thickness of the articular cartilage. Limitations of this animal model include the skeletal immaturity of the animal, as evidenced by the cartilaginous growth plate (Fig. 1). However, the selection of immature cartilage allowed for cartilage that was at least as thick as that of human adult cartilage. Additionally, the joint capsule was small enough to be kept intact within the bore of the high field strength MRI scanner.

While articular cartilage explants reach a steady-state load-deformation response in approximately 100 cycles, depending on the loading conditions (11), creep has been observed to continue in intact joints during cyclic loading (16). Therefore, defining a quasi-steady state condition allows for imaging with minimal motion artifacts and reasonable overall imaging times. The standard deviation of measured displacements also remained less than half the spatial resolution after a quasi-steady state was achieved.

Previous studies using DENSE-FSE in cartilage already have shown that the imaging sequence presents no significant displacement or strain bias (10). In this study, the displacement precision represents 26% of the spatial resolution of the sequence (i.e., 100 × 65 μm/250 μm), allowing for subpixel displacement resolution of the tissues of

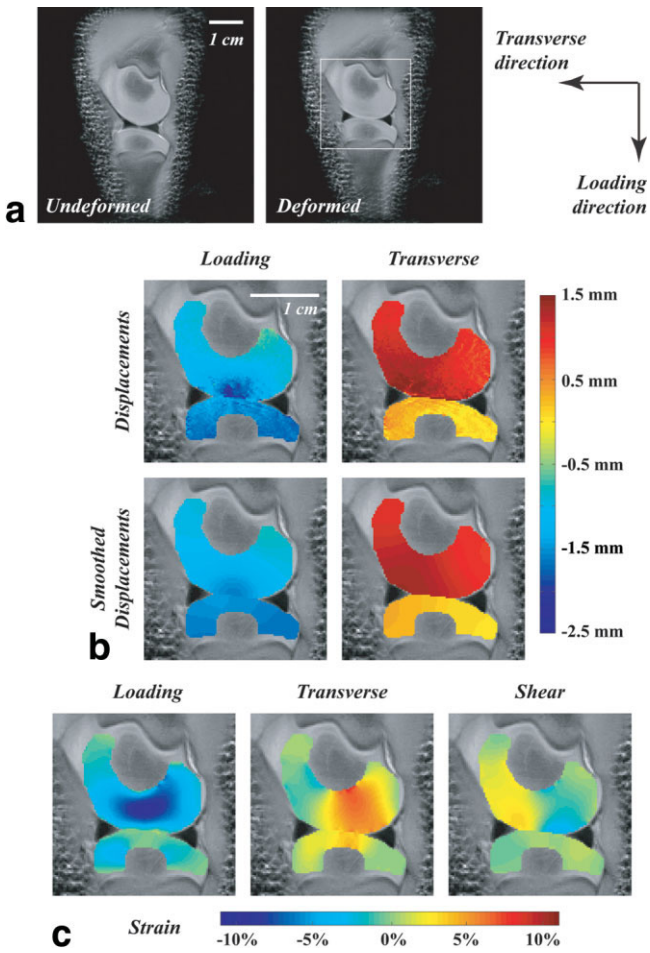


FIG. 5. Displacements and strains were complex and heterogeneous through femoral and tibial articular cartilage of an intact joint during simple compressive loading. Proton-weighted MR images of the undeformed and deformed porcine tibiofemoral joint are shown (**a**). The white box in A indicates the region that is magnified for subsequent MR images. The transverse and loading directions are defined as *x* and *y*, respectively, with the load applied in the negative *y* direction. Displacement data, both before and after smoothing, are shown for the loading and transverse directions (**b**). Strains in the loading direction in both the femur and tibia were negative and compressive (**c**).

interest. Smoothed displacements were negative in the loading direction, consistent with motion of the tibia in the direction of applied loading. Although the femoral shaft is held fixed in the apparatus, the cartilage in the growth plate is compressible, resulting in rigid body motion of the femur in the direction of loading. Displacements in the transverse direction indicate that the femoral articular cartilage moved in the anterior direction. This motion may be due to the shearing deformation of the growth plate cartilage, ligamentous and other soft tissue attachments, and the geometry of the opposing cartilage surfaces. It is important to note that the displacements measured are a combination of both rigid body motion and tissue deformation.

On the other hand, the strain data emphasize the deformation of the interior of the articular cartilage. Strains in the loading direction were compressive in both femoral and tibial cartilage. Additionally, positive transverse strains occurred in the femur and tibia, showing the expected Poisson's effect.

A significant strength of this work is the measurement of cartilage deformation in the interior of joint cartilage. A previous MRI study of articular cartilage measured average strains up to −7.2% in tibiofemoral cartilage following dynamic weight-bearing activities (9). However, the strains were based on the change in cartilage boundary thickness as determined by MRI. In contrast, the present work examined tissue deformation for each pixel of the imaged slice through the articular cartilage.

There are several limitations of the current DENSE-FSE imaging technique. A long preconditioning period was required before imaging to allow the articular cartilage to reach a quasi-steady state response. Although the signal-to-noise ratio in this study was comparable to a previous DENSE-FSE study (10), higher SNR will improve displacement precision. Low SNRs also affect image processing, requiring a more robust algorithm to correct and unwrap phase data. More rapid imaging sequences may reduce the preconditioning time by relaxing the steady-state criterion used herein and may improve the SNR by allowing for additional signal averaging in a fixed total imaging time. Lastly, a two-dimensional analysis was presented, allowing in-plane deformations to be computed. Extension of the technique to multiple slices is required to document full three-dimensional deformations throughout the joint.

Despite these limitations, the current study represents a step toward addressing specific biomechanics questions in vitro and eventually determining orthopedic tissue strains in vivo. In its present form, this technique may be applied in vitro to pathological joints, possibly providing insight into degeneration mechanisms. Data generated by the technique may be used to validate mathematical models of cartilage load-displacement response. Knowledge of the displacement environment of chondrocytes is also important in mechanobiology and tissue engineering. Future work may include improvement of the technique for use in a clinical MR scanner, measurement of heterogeneous strain fields in larger animal joints, and the adaptation of this technique for in vivo use in humans. Challenges in future work include increasing spatial resolution to allow imaging of thinner (e.g., osteoarthritic) articular cartilage and decreasing imaging time to allow for reasonable use in vivo.

In conclusion, this research has determined the heterogeneous displacements and strains within articular cartilage of a cyclically loaded intact joint. A loading apparatus was designed for use in a MRI scanner, and the precision of this technique was determined for various smoothing parameters. Despite limitations in imaging time and SNR, these results are useful in characterizing the deformation environment within an intact joint. Finally, this work constitutes an important step toward many potential biomechanics applications, including in vivo strain imaging of the articular cartilage of a load-bearing joint.

## REFERENCES


1. Butler DL, Goldstein SA, Guilak F. Functional tissue engineering: the role of biomechanics. J Biomech Eng 2000;122:570–575.
2. Guilak F, Butler DL, Goldstein SA. Functional tissue engineering: the role of biomechanics in articular cartilage repair. Clin Orthop Relat Res 2001;(Suppl):S295–S305.
3. de Crespigny AJ, Carpenter TA, Hall LD. Cardiac tagging in the rat using a DANTE sequence. Magn Reson Med 1991;21:151–156.
4. Young AA, Axel L, Dougherty L, Bogen DK, Parenteau CS. Validation of tagging with MR imaging to estimate material deformation. Radiology 1993;188:101–108.
5. Axel L, Dougherty L. MR imaging of motion with spatial modulation of magnetization. Radiology 1989;171:841–845.
6. Gold GE, Besier TF, Draper CE, Asakawa DS, Delp SL, Beaupre GS. Weight-bearing MRI of patellofemoral joint cartilage contact area. J Magn Reson Imaging 2004;20:526–530.
7. Herberhold C, Stammberger T, Faber S, Putz R, Englmeier KH, Reiser M, Eckstein F. An MR-based technique for quantifying the deformation of articular cartilage during mechanical loading in an intact cadaver joint. Magn Reson Med 1998;39:843–850.
8. Eckstein F, Lemberger B, Stammberger T, Englmeier KH, Reiser M. Patellar cartilage deformation in vivo after static versus dynamic loading. J Biomech 2000;33:819–825.
9. Eckstein F, Lemberger B, Gratzke C, Hudelmaier M, Glaser C, Englmeier KH, Reiser M. In vivo cartilage deformation after different types of activity and its dependence on physical training status. Ann Rheum Dis 2005;64:291–295.
10. Neu CP, Walton JH. Displacement encoding for the measurement of cartilage deformation. Magn Reson Med 2008;59:149–155.
11. Neu CP, Hull ML. Toward an MRI-based method to measure non-uniform cartilage deformation: an MRI-cyclic loading apparatus system and steady-state cyclic displacement of articular cartilage under compressive loading. J Biomech Eng 2003;125:180–188.
12. Poore KR, Forhead AJ, Gardner DS, Giussani DA, Fowden AL. The effects of birth weight on basal cardiovascular function in pigs at 3 months of age. J Physiol 2002;539(Pt 3):969–978.
13. Weinans H, Blankevoort L. Reconstruction of bone loading conditions from in vivo strain measurements. J Biomech 1995;28:739–744.
14. Epstein FH, Gilson WD. Displacement-encoded cardiac MRI using cosine and sine modulation to eliminate (CANSEL) artifact-generating echoes. Magn Reson Med 2004;52:774–781.
15. Geers MGD, de Borst R, Brekelmans WAM. Computing strain fields from discrete displacement fields in 2D-solids. Int J Solids Struct 1996; 33:4293–4307.
16. Martin KJ, Neu CP, Hull ML. An MRI-based method to align the compressive loading axis for human cadaveric knees. J Biomech Eng 2007; 129:855–862.